Characterization and elimination of stochastically generated persister subpopulation in mycobacteria

Vivek Srinivas[1], Mario Arrieta-Ortiz[1], Eliza J.R. Peterson[1*], Nitin S. Baliga[1-4]*

[1]Institute for Systems Biology, 401 Terry Ave N., Seattle WA 98109 USA.
[2]Departments of Biology and Microbiology, University of Washington, Seattle, WA, USA
[3]Molecular Engineering Program, University of Washington, Seattle, WA, USA
[4]Lawrence Berkeley National Lab, Berkeley, CA, USA

* Corresponding authors:
Eliza J.R. Peterson: epeterso@systemsbiology.org;
Nitin S. Baliga: nbaliga@systemsbiology.org

Highlights

- We have developed a novel method, Per-Sort, to isolate a small proportion of translationally dormant cells that pre-exist in *Mycobacterium spp.* cultures growing under optimal conditions but dramatically increase in proportion under stressful conditions.
- The pre-existing translationally dormant cells have lower oxygen consumption, significantly longer lag phase to initiate growth in nutrient rich medium, and high tolerance to >10x MIC concentrations of isoniazid (INH) and rifampicin (RIF), indicating they are a subpopulation of persister cells.
- Single-cell expression profiling demonstrated that the persisters are a heterogenous mixture of toxin (VapC30 and MazF) and alarmone response (RelA/SpoT) expressing cells.
- A shared outcome of high toxin and alarmone response is reduced cellular oxidative metabolism, which we demonstrate is reversed upon addition of L-cysteine to reduce the proportion of pre-existing persister cells and increase killing by INH and RIF.

Summary

Mycobacterium tuberculosis (MTB) is able to persist in the host for long periods of time, even during antibiotic treatment. Eliminating persister cells, which are implicated as the primary reason for treatment failure, is essential for shortening TB treatment regimen. Here, we report a novel methodology, Per-Sort, to identify and sort miniscule numbers of translationally dormant mycobacterial cells within an isogenic *mycobacterium* population. Using Per-Sort we have discovered that translationally dormant cells pre-exist (under optimal growth conditions) as a fraction of a percent of isogenic mycobacterial cultures, suggesting they are generated stochastically as a bet hedging strategy. We show that this pre-existing translationally dormant subpopulation of cells are tolerant to antibiotics, small in size, low in oxidative metabolism, and expand in number upon nutrient starvation. Finally, through transcriptional profiling at single cell resolution, we've determined that the pre-existing persisters are a heterogeneous mix of *vapC30*, *mazF*, and *relA/spoT* overexpressing cells that are eliminated and sensitized to antibiotic killing through induction of respiration.

Keywords: Mycobacterium, preexisting persisters, antibiotic tolerance, nutrient starvation

Introduction

Persister cells, a subpopulation of cells which are refractory to drug killing, are problematic to the chemotherapeutic treatment of tuberculosis (TB) disease. *Mycobacterium*

tuberculosis (MTB) persister cells are considered a major reason why a quarter of all TB patients require 6 months of treatment and 5% are not cured even then [1]. In addition to treatment failure, persister cells lead to recalcitrant infections [1,2] and the emergence of genetically-encoded drug resistance [3,4]. A better understanding of the intrinsic heterogeneity that leads to persister subpopulation(s) within a clonal population of mycobacteria is necessary to effectively treat persistent TB infections.

Persisters are drug tolerant bacteria, often associated with slow-growth and reduced metabolic activity [5,6]. However, the association between growth-arrest and persisters is currently a subject of intense debate. Importantly, persisters can re-establish drug sensitivity and normal growth upon culture in standard media. Resumption of normal growth is a key characteristic of persisters and distinguishes them from other antibiotic tolerant forms such as viable but non-cultivable cells (VBNCs) [7]. Given their similarity but important difference, VBNCs have obscured the characterization of persister cells; especially in studies using standard "persister assay" methods, which treat bacteria with antibiotics and collect the remaining non-lysed cells (considered persisters) by centrifugation. Therefore, we sought to establish a high-fidelity isolation technique to study mycobacteria that fit the fundamental definition of persisters, antibiotic tolerance and growth resumption in standard media. Furthermore, we sought a method that identified persisters independent of antibiotic selection, in other words, persisters that pre-exist in an isogenic culture in the absence of drugs (or other) pressure. Such pure fractions of persisters will enable an understanding of the processes for generating and maintaining diversity in mycobacteria.

Fluorescent reporters have enabled a repertoire of techniques to be developed and applied to study microbial community subpopulations, without the use of selection. In MTB, single-cell heterogeneity was captured *in vitro* and during murine infections using a reporter of 16s rRNA gene expression [8]. The microscopy-based platform was able to track heterogeneity in growth rate under standard growth conditions and found heterogeneity was amplified by stress conditions and murine infection. However, the non-growing subpopulation was not isolated and characterized further, most likely due to low fluorescence levels of the reporter. In another study, Jain *et al* developed a dual-reporter mycobacteriophage (ϕ^2DRM) system to sort and reveal pre-existing isoniazid (INH) tolerant MTB from *in vitro* cultures and human sputa [9]. Unfortunately, the necessity to re-infect daughter cells with ϕ^2DRM limited the ability to follow isolated cells over generations and study their regrowth patterns. Therefore, we designed an integrative inducible fluorescence reporter system that produced measurable fluorescence for isolation of heterogeneous subpopulations by cell sorting, and the ability to follow the population structure over generations. Previous studies have demonstrated that translation is suppressed in persisters, compared to actively growing cells [10,11]. In this study, we report a translation readout system based on an inducible fluorescent reporter that exploits this phenotypic trait to isolate and comprehensively characterize pre-existing, slow-growing persisters within a heterogeneous isogenic population of an actively growing mycobacterial culture. By performing single cell transcriptional profiling and phenotypic characterization of sorted mycobacterial subpopulations, we present evidence that persisters are generated

stochastically through a variety of mechanisms via a bet hedging strategy. We demonstrate that mycobacteria anticipate drug exposure upon sensing nutrient starvation to adaptively expand the persister cell subpopulation and proportionally increase drug tolerance. Finally, we demonstrate that notwithstanding the varied mechanisms by which persister cells are generated, they converge on a similar low oxygen (O_2) metabolic state that can be reversed through activation of respiration with cysteine to increase antibiotic susceptibility and eliminate persisters that are increased under physiological conditions.

Results and Discussion:

Per-Sort isolates pre-existing translationally dormant *Mycobacterium* cells that are antibiotic tolerant

To identify translationally heterogeneous subpopulations in mycobacteria, we generated a reporter plasmid with mEos2 fluorescent reporter[12] under the transcriptional control of an anhydrotetracycline (ATc) inducible promoter and a strong mycobacterial translation initiation signal (trans-mEos2). The plasmid also encoded an integrase gene for chromosomal integration in *Mycobacterium spp.* genomes (see methods). The reported plasmid was transfected into *Mycobacterium smegmatis* (mc^2155) (MSM-mEos2) and fluorescence-activated cell sorting (FACS) was used to differentiate single mycobacterial cells based on mEos2 fluorescence level. Cell sorting was optimized using a mixed culture of ATc induced MSM-mEos2 cells (resistant to kanamycin) and MSM cells expressing mCherry (resistant to hygromycin) [13] with 1 µm beads for calibration. Cells from the mixed cultures were sorted and plated onto 7H10 plates with appropriate antibiotic selection. We observed a separation efficiency of 95% (**Fig S1a**), demonstrating our FACS sorting method reports on population structure and not an artifact of cell clumping [14]. We further defined gates for mEos2 fluorescing and non-fluorescing cells using heat killed and non-induced cells (**Fig S1b**). Using the optimized FACS method and MSM-mEos2 reporter strain, we found that post-induction with ATc, a majority of the overall population had fluorescence ("lit" cells), while a small fraction (<1%) were non-fluorescing ("dim cells", **Fig 1a**).

To confirm that the dim and lit cells have similar mEos2 transcript levels and that the difference in fluorescence is due to variation in translation rate, we isolated mRNA from 300,000 cells from each sorted dim and lit subpopulations. We quantified mEos2 transcript levels by qRT-PCR, using the constitutive expression of the kanamycin selection gene for normalization. The mEos2 transcript levels were not significantly different between the dim and lit subpopulations (**Fig 1b**), confirming that the absence of fluorescence in the dim cells is likely due to reduced rate of translation.

Next, in order to ascertain that there were no VBNCs within sorted dim and lit cells, we assayed their viability by sorting 10,000 cells from each subpopulation (including dead cells as

control), and plated 1:100 dilution onto 7H10 plates. The percentage of cultivable cells was identical (90%) across the dim and lit populations, confirming that neither population was over-represented with VBNCs (**Fig 1c**). We further investigated characteristics of regrowth of dim and lit cells by sorting 1000 cells of each subpopulation into 7H9 media. When the cultures reached an OD_{600} of 0.6, the expression of mEos2 was induced by addition of ATc and incubation for 12 hours, thereafter the cultures were re-analyzed by flow cytometry. Cultures generated from both dim and lit subpopulations had similar structure as the parent population vis-à-vis proportions of dim and lit cells, 99.5% lit cells and 0.5% dim cells (**Fig 1d**). These results demonstrated that translational dormancy of dim cells is not heritable and that the population structure is generated stochastically with dim and lit cells dividing to produce daughter cells of each type at a fixed probability (dim cells @p=0.05, and lit cells @p=0.95) under optimal growth conditions.

We investigated drug susceptibility of dim and lit subpopulations, given the known relationship between phenotypic heterogeneity and drug tolerance [8,15,16]. Using FACS, we sorted 10,000 cells each of the dim and lit subpopulations into 7H9 media containing ~10x MIC of isoniazid (INH) or rifampicin (RIF) for 8 hours. The cells were incubated at 37°C with antibiotic for 8 hours, washed in 7H9 media and dilutions plated onto 7H10. By comparing CFUs from the subpopulations before and after antibiotic treatment, we observed that a significantly greater proportion of dim cells survived in the presence of high concentrations of INH and RIF (**Fig 1e**), demonstrating that the translationally dormant dim cells are refractory to antibacterial killing. Further, these results demonstrate that translationally dormant, drug tolerant persisters pre-exist in small numbers (<0.5%) within an isogenic population of MSM growing under optimal growth conditions. Importantly, the results also demonstrate the capability of the Per-Sort technology to identify and sort these translationally dormant persisters, even though they exist as a tiny fraction of the overall population. We demonstrated that this technology is generalizable to other mycobacteria by performing Per-Sort with MTB transformed with the trans-mEos2 reporter. We observed similar translational heterogeneity and a similar size subpopulation of pre-existing INH tolerant persisters under optimal growth conditions (**Fig S2**).

Translationally dormant pre-existing persisters are characterized by small size, reduced respiration and longer lag phase.

While performing Per-Sort, we observed that intensity of side scatter by dim cells (SSC) was lower relative to lit cells, indicating they were smaller in size relative to lit cells (**Fig 2a**). Further, size distribution of dim cells was narrow across the subpopulation with >95% of the cells measuring <1 µm, whereas the size distribution of lit cells spanned from < 1 µm to > 3.5 µm (**Fig S3a**). The small size morphology of the dim cells is comparable to the 1 µm small resting cells (SMRCs) of MSM discovered during gentle starvation [16]. In addition to small size, SMRCs

were found to have extreme antibiotic tolerance and reduced metabolic activity [16]. Therefore, we assayed the level of oxidative metabolism within dim and lit cells with Per-Sort and estimated relative Reactive Oxygen Species (ROS) levels within each subpopulation using the ROS indicator dye CellROX orange. The positive control for this study (i.e., ROS+ cells) was generated by triggering ROS production across the ATc induced MSM-mEos2 culture by adding tert-butyl hydroperoxide. Similarly, a negative control was also included by treating the ATc induced MSM-Eos2 culture with N-acetyl-cysteine to quench ROS (**Fig 2b**). The lower CellROX orange fluorescence of dim cells compared to lit cells, indicated that dim cells had low ROS levels (we show later that this is potentially because of a subdued citric acid (TCA) cycle, a major source of ROS [17]).

As previously shown by Wu *et al*, SMRCs grow out to 'large' cells before resuming normal cell division, exhibiting a lag phase of 6 h without increase in CFUs during regrowth [16]. To look at the regrowth properties of the dim and lit subpopulations, we used an adaptation of ScanLag, a technique that combines cell plating with high-throughput dynamic imaging [18]. Per-Sorted dim and lit cells (100 cells) were plated onto 7H10 media and observed via ScanLag for 3 days and pictures were taken at the interval of 90 mins. Colonies from the lit population were collected from both the high and low mEOS2 fluorescence intensity spectrum. Regardless of the relative translational status of cells (i.e., fluorescence intensity), the time of appearance (TOA) of colonies from lit cells was the same (**Fig 2c**), indicating that this subpopulation was phenotypically uniform with respect to growth. By contrast, TOA of colonies from dim cell subpopulation occurred over a broader time range and on average 10 h after the lit cells (**Fig 2c**). The longer lag phase of the dim cells was reproduced in liquid cultures, wherein growth was monitored by recording absorbance (OD_{600}) at 30 m intervals for 3 days (**Fig S3b**). However, there was no difference in maximum growth rate between dim and lit cultures (OD_{600} slope = 0.12 Hr^{-1} for both) once cell division resumed. Delayed growth resulting from an extended lag time is a phenotype well-established with drug tolerance [4,19].

Nutrient starvation increases proportion of translationally dormant persister cells

The striking similarities between SMRCs and dim cells led us to hypothesize that dim cells are a phenotypically distinct subpopulation of cells that pre-exist in the bulk population to ensure survival in fluctuating environments. If so, we predicted that the proportion of dim cells in the population would increase in response to environmental change, such as starvation and drug pressure. To test this, MSM-mEos2 cells were grown in 7H9 media with varying amounts of glycerol (0.5% and 0.001%), until cultures reached exponential growth. We then induced the cultures with ATc and performed Per-Sort on half of the sample and the other half of the starved culture was treated with 10x MIC of INH and 5x MIC of RIF for 12 hours and assessed for antibiotic survival, as described previously in **Fig 1e**. Analysis by Per-Sort discovered a 10-

fold increase in dim cells induced by starvation (**Fig 3a**). The starvation-induced increase in dim cell proportion was also associated with a proportional increase in tolerance to INH in the bulk population (**Fig 3b**). We also grew MSM cells in 7H9 media with standard (0.5% v/v) or low (0.005% v/v) glycerol until the cultures reached saturation. We diluted and plated aliquots of these cultures onto 7H10 media (0.5% glycerol) and used ScanLag to observe regrowth properties. Cultures grown in standard glycerol media had two subpopulations with a 10 hour difference in their TOA (**Fig S4)**. This was consistent with the lag phase difference between the dim and lit subpopulations, confirming the presence of pre-existing persister cells in standard growth conditions. However, cultures starved of nutrients (0.005% glycerol) displayed a uniform delayed TOA (10 h), indicating the expansion of the persister cell population in nutrient starved conditions (**Fig S4**).

We also tested whether the dim cell numbers expand in response to low dose drug pressure, to investigate if this phenomenon could be attributed to generalized stress that was common to antibiotic exposure and nutrient starvation. Instead of transfer to PBS, the MSM-mEos2 cultures were mildly stressed with 0.1x MIC of INH. The INH pre-treatment only slightly increased the proportion of dim cells (2-fold increase shown in (**Fig S4**), but had a significant increase in the bulk tolerance to INH and RIF (Fig S4b). Interestingly, INH treatment led to higher variance in mEos2 fluorescence and shift in bulk population towards translational dormancy, as indicated by reduced mEos2 fluorescence intensity from the INH treated culture, compared to untreated (**Fig 3c**). Thus, the response to low dose INH response is distinct relative to nutrient starvation, which resulted in a clear bimodal distribution of fluorescence intensity and a dramatic increase in the dim cell subpopulation (**Fig 3d**). These data suggest that nutrient starvation and sub-MIC INH treatment increase antibiotic tolerance via distinct mechanisms. While the former induces an expansion of persister cells, the latter induces the formation of an intermediate adaptive state that affords antibiotic tolerance and perhaps better fitness in the presence of mild drug pressure. The bimodal distribution observed under nutrient starvation is characteristic of stochastic switching between two distinct phenotypes [20-22]. While the rate of stochastic switching under optimal growth conditions preferentially generates a fast growing, translationally active, and INH susceptible population (i.e., the lit cells), nutrient starvation shifts the dynamics of switching towards a slow growing, translationally dormant, and INH tolerant subpopulation (*i.e.*, the dim persister cells) (**Fig 3d**).

Noise in expression of *vapC30*, *mazF* toxins, or *relA/spoT* alarmone response induces the stochastic formation of translationally dormant persisters

The observation that persisters pre-exist within isogenic cultures of mycobacteria suggests that they might be stochastically generated by noise in gene expression at the single-cell level as a fail-safe measure against unpredictable environmental stressors [23,24]. While this

phenomenon is well-known in other pathogenic and non-pathogenic bacteria, it has never before been implicated in formation of persisters in isogenic mycobacterial cultures, in absence of drug pressure [25,26]. Therefore, we profiled within individual cells of both dim and lit subpopulations, the transcript levels of 45 genes that were previously implicated in persister formation in *Mycobacterium* spp. and *E. coli* (**Table S1**). Single-cell gene expression profiling was performed with the Fluidigm Biomark 48x48 system per manufacturer instructions and assayed relative to single-cell genomic DNA signal [27]. Transcript abundance was also normalized to a spike-in RNA control to account for experimental noise.

Kernel PCA (kPCA) with RBF (radial basis function) kernels [28] was used to identify the groups among dim and lit subpopulation based on patterns in their persister genes expression and toxin:antitoxin ratio, since toxins induce persister formation when they are expressed at higher levels relative to their antitoxin counterpart [29]. The kPCA identified overlapping clusters demonstrating phenotypic uncertainty from expression of persister genes (**Fig4a**). Unlike the lit cell subpopulation that had a unimodal spread, histograms plotted on the principal component with highest variance revealed three modes (transcriptional subgroups) in the dim cell subpopulation. As features are transformed onto a nonlinear state space in kPCA, their role in grouping is difficult to analyze. Therefore, we performed hierarchical clustering [30] of single-cell transcriptomes and reproduced the tripartite sub-grouping. Hierarchical clustering of cells with elevated *relA/spoT* transcript level and increased toxin to antitoxin ratio (*vapC30:B30* and *mazF:E*) stratified dim cells into three statistically significant clusters with at least four cells per cluster (approximately unbiased p-value >90) (**Fig 4b, S5**). Importantly, we did not detect similar population stratification through clustering analysis of lit cell transcriptomes (**Fig 4b**, **S5d**) mirroring the observations in kPCA analysis (**Fig 4a**). Further, whereas 80% of dim cells (20/25) were associated with elevated transcript levels of *relA/spoT* ($\geq \log_2 3.5$), high *mazF:E* ratio ($\geq \log_2 0.7$), or *vapC30:B30* ratio ($\geq \log_2 0.7$), only 35% (9/26) of the lit cells had similar associations. These data suggest that high expression of RelA/SpoT and presence of free toxins VapC30, and MazF might be responsible for higher rate of persister formation in the dim cell subpopulation.

Next, we sought further evidence that one or some combination of the three mechanisms were indeed active in dim cell subpopulation and the likely mechanism(s) for persister formation. The VapC30 and MazF toxins belong to a family of type II toxin-antitoxin (TA) systems, implicated in mycobacterial dormancy and persistence [31-33]. Activation of the type II TA system results in toxin-mediated cleavage of specific mRNAs [34], tRNAs [35], or rRNAs [35,36] causing translational dormancy [37]. Since the specific target mRNAs and tRNAs of VapC30 and MazF were unknown, we analyzed 16S and 23S rRNA levels in dim and lit cells by qRT-PCR. We discovered that dim cells have lower rRNA content relative to lit cells; and we did not observe the same pattern with a transcript level of a highly expressed metabolic gene (phosphoglucoisomerase, *pgi*) (**Fig 4c**). These data support the hypothesis that translational

dormancy in dim cells with high *vapC30:vapB30* and *mazF:mazE* ratios are a consequence of toxin-mediated cleavage of rRNA.

The RelA/SpoT protein, on the other hand, controls the so-called "alarmone response", which acts to resist various stresses, including oxidative stress and nutrient starvation [38]. Briefly, RelA/SpoT is bifunctional, capable of both synthesizing and hydrolyzing (p)ppGpp [39], an alarmone metabolite known to be required for long-term survival of mycobacteria during nutrient starvation [40-42], persistence of MTB in mice [43], and has been shown to induce the formation of persister cells in *E. coli* [37,44]. We discovered two lines of evidence to support the hypothesis that RelA/SpoT is predominantly in a synthase form within the dim cell subpopulation. First, significant number of cells (8/13) expressing high levels of *relA/spoT* are also associated with high *mazF:mazE* ratio, suggesting that the RelA/SpoT system might be acting through (p)ppGpp-mediated inactivation of the MazE antitoxin in these cells. Second, we observed only within dim cells a significant correlation (R= 0.89, p-value=0.001) between *relA/spoT* transcript levels and 6 alarmone response transcripts, all of which are implicated as drivers of dormancy (**Table S1**).

Elimination of translationally dormant persisters reduces antibiotic tolerance and potentiates drug activity

Our data suggest that stochastic activation of at least three mechanisms may be responsible for generating translationally dormant persister cells in isogenic mycobacterial cultures growing under optimal conditions (**Fig 1**). We further hypothesize that the dynamics of these stochastic mechanisms shift in response to host-derived stress (*i.e.* nutrient starvation), leading to an increase in the proportion of persister cells (**Fig 3**). As such, blocking these mechanisms could potentially prevent the formation of both pre-existing and stress-induced persister cell populations, leading to improvement in drug treatment outcome. However, the multiplicity of mechanisms that could be deployed in a combinatorial scheme confounds this strategy (e.g., MTB genome encodes >70 TA systems). Furthermore, we are yet to discover drugs that can specifically target TA systems or drugs that can kickstart translation. Notwithstanding these confounding issues, metabolic pathway analysis (see methods) from GSE29631, GSE69681, and GSE69983 GEO gene expression microarray datasets belonging to VapC30 over expression, RelA/SpoT knockout under nutrient starvation and nutrient starvation respectively suggests that the multiplicity of mechanisms for persister formation all converge into a physiologic state associated with reduced TCA cycle, which is consistent with the low ROS levels in cells of this subpopulation (**Fig 3b and 5a**). Therefore, we explored the use of L-cysteine to increase oxygen consumption in the translationally dormant persisters. L-cysteine was previously shown to convert MTB persister cells (selected in the presence of INH) to actively oxygen respiring cells and potentiate INH and RIF killing [45]. In accordance with their results, MSM cultures grown to

mid-log phase in presence of 4mM L-cysteine were assayed by Per-Sort and found to be completely devoid of dim cells (**Fig 5b**). Importantly, our data goes beyond the previous study by demonstrating that promoting oxidative metabolism can eradicate pre-existing persister cells that form independent of drug pressure. We also found that treatment with L-cysteine increased INH and RIF susceptibility of the bulk population by 100-fold, compared to nutrient starvation conditions (**Fig 5c**). Nutrient starvation conditions, which activate RelA/SpoT induced alarmone response [46] act in opposition to L-cysteine by increasing the proportion of dim cells (**Fig 5b**), and thus increasing drug tolerance of the entire population (**Fig 5c**) and MDK_{95} (minimum duration for killing 95% of bacterial cells) of RIF (**Fig 5d**). Furthermore, L-cysteine significantly reduced the MDK_{95} of RIF in nutrient starved cultures (**Fig 5d**). Ultimately, these results demonstrate the potential of strategies to eliminate pre-existing persisters to improve the treatment of TB.

Conclusions

Numerous studies have revealed cell-to-cell variability in organisms from all domains of life –unicellular to multicellular. Phenotypic variation confers fitness advantage to pathogens such as MTB, which routinely experience varying and hostile environments within the host. Through cell-to-cell variability, the population is able to prepare for a probable new environment by harbouring a subpopulation that is pre-adapted to that environment. Unfortunately, this evolutionary strategy, called bet-hedging, impedes the ability to effectively treat TB due to the presence of drug tolerant persister cells. In this study, we developed a method to identify drug-tolerant persisters in MSM culture. The characterization of such persisters could facilitate the means to shorten TB treatment.

Using Per-Sort we isolated a translationally dormant subpopulation based on the absence of mEos2 fluorescence after induction of transcriptional overexpression of the reporter with ATc. In addition to INH and RIF tolerance, this “dim” persister subpopulation was demonstrated to be small in size, have reduced oxygen metabolism and a longer lag phase upon regrowth. Such properties are consistent with that of small morphotype resting cells (SMRCs), formed during mild nutrient starvation [16]. Here we report these cells actually pre-exist in low numbers in a isogenic MSM culture growing under optimal low stress conditions. We believe these cells, and likely other phenotypically heterogeneous subpopulations, are generated and maintained to withstand complex and unpredictable environmental stress.

Upon nutrient starvation, we discovered there is a significant increase in the proportion of translationally dormant persister cells and a clear bimodal distribution of dim and lit cells (Fig 3a). These results are indicative of a shift in dynamics of stochastic phenotypic switching that favors expansion of the subpopulation in a translationally dormant phenotype in nutrient starved conditions. This begs the question of what is being stochastically altered in less than 1%

of the population and influencing the translational state of this mycobacterial subpopulation. Most often diversity is generated within a clonal population by stochastic processes that introduce noise in gene expression at the single-cell level [47-49]. We have overcome the challenge of characterizing persisters at single cell resolution by sorting them and not by killing the susceptible cells with antibiotics. This technological advancement has overcome the confounding issue that the antibiotic treatment itself might induce persister cell formation, which we demonstrate with 0.1X MIC INH treatment (**Fig 3**). Further, our technology allows comparative analysis of persister cells *and* actively growing drug susceptible cells from the *same* culture. Because of these novel capabilities of Per-Sort, we were able to quantify transcript abundance of 45 genes associated with persister formation and drug tolerance in 45 single cells from both dim and lit subpopulations. Expression analysis revealed that stochastic activation of TA systems and dual-functionality of RelA/SpoT are the basis of translationally dormant persister formation in MSM cultures. These results reinforce the hypothesis that there are multiple pathways to become a persister cell and reveal the complex and combinatorial schemes used by mycobacteria to generate heterogeneous subpopulations.

Among the dim cells, we found that high expression of toxin *mazF* was also associated with high *relA/spoT* expression. We suspect that MazEF can be activated by the alarmone response, elicited by RelA/SpoT synthesis of (p)ppGpp, in a manner similar to the well-studied *hipAB* of *E. coli* persisters [50]. In contrast, the single-cell expression data suggest that VapC30 can act to induce persister formation in an alarmone-independent mechanism. This supports a recent study demonstrating that a *relA/spoT* knockout mutant of MSM, with reduced alarmone response, still formed persisters against INH and ciprofloxacin at levels similar to wildtype [51]. Indicating multiple mechanisms of persister formation exist in mycobacteria, some of which are independent of RelA/SpoT, and might be controlled by VapC30 activation. While MSM has a single VapBC-type TA system, MTB has 70 copies of VapBC, indicating the pathogen has evolved to increase phenotypic diversity and bet-hedging for survival in the host environment. Much work is still needed to understand how and when these mechanisms are activated, and whether the resulting subpopulations have distinct or generalized drug tolerance.

In addition to posttranscriptional cleavage of rRNA and reducing translation in a subpopulation of cells, activation of TA systems and the alarmone response has been shown to decrease oxidative metabolism in persisters [34,52]. Similarly, we demonstrated lower ROS levels in the dim cells compared to lit cells, indicating reduced oxygen consumption in the translationally dormant persister cells. As such, both translation and oxidative metabolism are processes that could be targeted to modulate this subpopulation. We confirmed by demonstrating that addition of L-cysteine, which is known to activate cellular oxidative metabolism, dramatically reduced the proportion of translationally dormant persisters in actively growing MSM cultures. As such, when used with a drug, L-cysteine potentiates faster drug killing by increasing the oxidative metabolism of the pre-existing persister cell population

and thereby increasing their drug susceptibility. However, L-cysteine is a metabolite and cannot be used for treatment *in vivo*. Therefore, other strategies that activate oxidative pathways similar to L-cysteine (i.e. cis-2-decenoic acid [53] or superoxide-producing nanoparticles [54]) or activate translation should be tested. Alternatively, our study also proposes inhibition of VapC30 and RelA/SpoT synthase activity (such as (p)ppGpp analogs like relacin [55]) would block persisters from forming *a priori*. This study highlights how mechanistic knowledge will enable targeted strategies to eliminate detrimental persisters, thereby shortening the course of treatment and preventing the emergence of resistance.

Materials and methods-

Bacterial growth and MSM-mEos2 strain development: *M. smegmatis* MC155 strains (MSM) were obtained from ATCC and grown in 7H9 broth medium (Difco) with 0.2% glycerol, 0.05% tween, and 10% ADC enrichment (BD biosciences). pSTKi-mEos2 plasmid were constructed from pSTKi plasmid [56] , and pRSETa mEos2 plasmid [57]. Synthetic oligo with translation initiation signal (mycoSD) was used to amplify mEos2 from pRSETa mEos2 plasmid, amplified fragment was inserted into the pSTKi plasmid with restriction ligation at BamH1 and EcoR1 sites. pSTKi-mEos2 transcript was electroporated into the electrocompetent MSM cultures, transformed colonies were selected on 7H10 plates with 30 µg/ml kanamycin (KAN). MSM-mEos2 cells were cultured in 7H9 media with 30 µg/ml KAN.

Development of per-SORT: per-SORT was developed in BD FACS Influx, 70 micron tip and sheath fluid from BD bioscience was used in sorting and FACS analysis. Fluorescence beads (1, 3.5 micron green fluorescence, and Accudrop) from BD biosciences was used to calibrate the instrument for laser alignment, compensation, and cell sorting. Propidium Iodide (PI) stain (SigmaAldridge, 5µl/1ml) was used to stain dead cell. Heat killed cells (incubated at $70^{o} – 80^{o}$ C for 5 mins) was used to prepare dead cell control for PI stain. MSM cells with pCHERRY3 plasmid [58] (MSM-mCherry) was used to optimize single cell mycobacterium sorting. MSM-mEos2 (KAN resistant) cultures induced with 25ng/ml ATc and MSM-mCherry (Hygromycin resistant) were mixed in equal proportions. Single cell sorting efficiency was determined by plating sorted cells on 7H10 plates with KAN and HYG. Gates for sorting dim and lit cells of ATc induced MSM-mEos2 strains were determined using uninduced MSM-mEos2 strains stained with PI. FACS data was analyzed in FlowJo ver. 10 software.

Antimicrobial tolerance assay: Minimum inhibitory concentrations (MIC) of the MSM-mEOS2 strains were determined with disk diffusion assay [59] . Cultures (bulk, per-Sorted) were incubated in 7H9 media containing desired MIC concentrations of INH and RIF. Drug treated bacteria were washed with or diluted (1:100) in 7H9 media and plated (100 µl) or spotted (5 µl) on 7H10 media with 30 µg/ml KAN at time points 0, 8, 12, 16, 20, and 24 hours after incubation. Percentage survival was calculated with respect to 0 hours.

Single cell persister gene expression and analysis: Fluidigm Biomark system with 48x48 plates were used for this analysis. Single dim and lit cells were per-Sorted into 96 well plates with

VILO™ reaction mix (5x), SUPERase (Invitrogen™), and 10% NP40 in an pre-noted random order to avoid sampling bias. Sorted plates were spun down and freeze-thawed 3 times on dry ice to rupture cells. Assay for non-transcribed genomic DNA (Table S1) was used to determine the rupture efficiency. Reverse transcription (RT) was performed on freeze thawed cells with VILO cDNA preparation mixture, T4-Gene32 protein, and random hexamer primers. RNA spike-in (ECC2_SpikeIn RNA, 10 pM) was included in the RT master mix. cDNA of the genes of interest (Table S1) was pre-amplified with TaqMan® PreAmp master mix (Invitrogen™) and equimolar mixture of forward and reverse strand primers designed for the genes of interest (Table S2). Primers were removed with Exonuclease I (Invitrogen™). Primers sets used for preamplification (Table S2) were primed into the 48x48 Biomark assay plates. Quantitative PCR assay with Biomark prescribed protocol was run on diluted, pre-amplified Exo 1 treated cDNA with Sso Fast EvaGreen Supermix (Bio-Rad laboratories). Quality control for determining, sorting, cell lysis, and cDNA preparation was performed by comparing the CT values of genomic DNA control and spike-in control in all the cells. Expression levels of genes was measured as ∂CT in individual cells with reference to genomic DNA control (expected to result from 1 copy of genomic DNA), less than or equal expression (of genomic DNA control) was considered as zero expression and assays with CT >45 were flagged as missing values. ∂CT values for each cells were corrected by adding or subtracting the deviation from median ∂CT of spike-in control for a particular cell. Hierarchical clustering was performed with Seaborn package of Python and PVclust package of R.

Pathway analysis: Gene expression data sets of VapC overexpression (GSE29631), RelA/SpoT knockout in nutrient starvation (growth in PBS, GSE69681), and nutrient starvation (growth in PBS, GSE69983) was obtained from GEO database and analysed with Cyber-T tool [60] to identify differentially expressed genes (DEG) in the respective conditions. DEG was mapped onto the central carbon metabolism of MSM with the gene annotations obtained from KEGG pathways. DEGs in GSE69983 which significantly deviated from GSE69681 were considered to be the changes caused by RelA/SpoT induced alarmone response.

Acknowledgements: We thank members of the Baliga lab for critical discussions; Amardeep Kaur for her technical expertise; Tim Petersen and Monica Orellana for help with FACS; Seattle Children's Research Institute, particularly David Sherman, Christoph Grundner and Weldon DeBusk for BSL-3 access and help. Funding was provided by the National Institute of Allergy and Infectious Diseases of the National Institutes of Health [R01 AI128215] and [U19 AI10676, U19 AI135976]; and National Science Foundation [1518261, 1565166, and 1616955].

Author contributions: V.S. designed research, performed research, analyzed data and wrote the paper. M.A. performed computational analyses. E.J.R.P and N.S.B. designed research, analyzed data, and wrote the paper.

Competing interests: The authors declare no competing financial interests.

References

1. Sarathy JP, Via LE, Weiner D, Blanc L, Boshoff H, Eugenin EA, Barry CE, 3rd, Dartois VA. Extreme Drug Tolerance of Mycobacterium tuberculosis in Caseum. Antimicrob Agents Chemother. 2018;62(2). doi: 10.1128/AAC.02266-17. PubMed PMID: 29203492; PMCID: PMC5786764.
2. Connolly LE, Edelstein PH, Ramakrishnan L. Why is long-term therapy required to cure tuberculosis? PLoS Med. 2007;4(3):e120. doi: 10.1371/journal.pmed.0040120. PubMed PMID: 17388672; PMCID: PMC1831743.
3. Cohen NR, Lobritz MA, Collins JJ. Microbial persistence and the road to drug resistance. Cell Host Microbe. 2013;13(6):632-42. doi: 10.1016/j.chom.2013.05.009. PubMed PMID: 23768488; PMCID: PMC3695397.
4. Levin-Reisman I, Ronin I, Gefen O, Braniss I, Shoresh N, Balaban NQ. Antibiotic tolerance facilitates the evolution of resistance. Science. 2017;355(6327):826-30. doi: 10.1126/science.aaj2191. PubMed PMID: 28183996.
5. Amato SM, Fazen CH, Henry TC, Mok WW, Orman MA, Sandvik EL, Volzing KG, Brynildsen MP. The role of metabolism in bacterial persistence. Front Microbiol. 2014;5:70. doi: 10.3389/fmicb.2014.00070. PubMed PMID: 24624123; PMCID: PMC3939429.
6. Helaine S, Cheverton AM, Watson KG, Faure LM, Matthews SA, Holden DW. Internalization of Salmonella by macrophages induces formation of nonreplicating persisters. Science. 2014;343(6167):204-8. doi: 10.1126/science.1244705. PubMed PMID: 24408438.
7. Orman MA, Henry TC, DeCoste CJ, Brynildsen MP. Analyzing Persister Physiology with Fluorescence-Activated Cell Sorting. Methods Mol Biol. 2016;1333:83-100. doi: 10.1007/978-1-4939-2854-5_8. PubMed PMID: 26468102; PMCID: PMC4908830.
8. Manina G, Dhar N, McKinney JD. Stress and host immunity amplify Mycobacterium tuberculosis phenotypic heterogeneity and induce nongrowing metabolically active forms. Cell Host Microbe. 2015;17(1):32-46. doi: 10.1016/j.chom.2014.11.016. PubMed PMID: 25543231.

9. Jain P, Weinrick BC, Kalivoda EJ, Yang H, Munsamy V, Vilcheze C, Weisbrod TR, Larsen MH, O'Donnell MR, Pym A, Jacobs WR, Jr. Dual-Reporter Mycobacteriophages (Phi2DRMs) Reveal Preexisting Mycobacterium tuberculosis Persistent Cells in Human Sputum. MBio. 2016;7(5). doi: 10.1128/mBio.01023-16. PubMed PMID: 27795387; PMCID: PMC5080378.
10. Cho J, Rogers J, Kearns M, Leslie M, Hartson SD, Wilson KS. Escherichia coli persister cells suppress translation by selectively disassembling and degrading their ribosomes. Mol Microbiol. 2015;95(2):352-64. doi: 10.1111/mmi.12884. PubMed PMID: 25425348.
11. Shah D, Zhang Z, Khodursky A, Kaldalu N, Kurg K, Lewis K. Persisters: a distinct physiological state of E. coli. BMC Microbiol. 2006;6:53. doi: 10.1186/1471-2180-6-53. PubMed PMID: 16768798; PMCID: PMC1557402.
12. McKinney SA, Murphy CS, Hazelwood KL, Davidson MW, Looger LL. A bright and photostable photoconvertible fluorescent protein. Nat Methods. 2009;6(2):131-3. doi: 10.1038/nmeth.1296. PubMed PMID: 19169260; PMCID: PMC2745648.
13. Carroll P, Schreuder LJ, Muwanguzi-Karugaba J, Wiles S, Robertson BD, Ripoll J, Ward TH, Bancroft GJ, Schaible UE, Parish T. Sensitive detection of gene expression in mycobacteria under replicating and non-replicating conditions using optimized far-red reporters. PLoS One. 2010;5(3):e9823. doi: 10.1371/journal.pone.0009823. PubMed PMID: 20352111; PMCID: PMC2843721.
14. Tracy BP, Gaida SM, Papoutsakis ET. Flow cytometry for bacteria: enabling metabolic engineering, synthetic biology and the elucidation of complex phenotypes. Curr Opin Biotechnol. 2010;21(1):85-99. doi: 10.1016/j.copbio.2010.02.006. PubMed PMID: 20206495.
15. Wakamoto Y, Dhar N, Chait R, Schneider K, Signorino-Gelo F, Leibler S, McKinney JD. Dynamic persistence of antibiotic-stressed mycobacteria. Science. 2013;339(6115):91-5. doi: 10.1126/science.1229858. PubMed PMID: 23288538.
16. Wu ML, Gengenbacher M, Dick T. Mild Nutrient Starvation Triggers the Development of a Small-Cell Survival Morphotype in Mycobacteria. Front Microbiol. 2016;7:947. doi: 10.3389/fmicb.2016.00947. PubMed PMID: 27379076; PMCID: PMC4909757.
17. Kohanski MA, Dwyer DJ, Hayete B, Lawrence CA, Collins JJ. A common mechanism of cellular death induced by bactericidal antibiotics. Cell. 2007;130(5):797-810. doi: 10.1016/j.cell.2007.06.049. PubMed PMID: 17803904.
18. Levin-Reisman I, Fridman O, Balaban NQ. ScanLag: high-throughput quantification of colony growth and lag time. J Vis Exp. 2014(89). doi: 10.3791/51456. PubMed PMID: 25077667; PMCID: PMC4215631.
19. Fridman O, Goldberg A, Ronin I, Shoresh N, Balaban NQ. Optimization of lag time underlies antibiotic tolerance in evolved bacterial populations. Nature. 2014;513(7518):418-21. doi: 10.1038/nature13469. PubMed PMID: 25043002.
20. Kussell E, Leibler S. Phenotypic diversity, population growth, and information in fluctuating environments. Science. 2005;309(5743):2075-8. doi: 10.1126/science.1114383. PubMed PMID: 16123265.
21. Acar M, Mettetal JT, van Oudenaarden A. Stochastic switching as a survival strategy in fluctuating environments. Nat Genet. 2008;40(4):471-5. doi: 10.1038/ng.110. PubMed PMID: 18362885.

22. Kotte O, Volkmer B, Radzikowski JL, Heinemann M. Phenotypic bistability in Escherichia coli's central carbon metabolism. Mol Syst Biol. 2014;10:736. doi: 10.15252/msb.20135022. PubMed PMID: 24987115; PMCID: PMC4299493.
23. Eldar A, Elowitz MB. Functional roles for noise in genetic circuits. Nature. 2010;467(7312):167-73. doi: 10.1038/nature09326. PubMed PMID: 20829787; PMCID: PMC4100692.
24. Choi PJ, Cai L, Frieda K, Xie XS. A stochastic single-molecule event triggers phenotype switching of a bacterial cell. Science. 2008;322(5900):442-6. doi: 10.1126/science.1161427. PubMed PMID: 18927393; PMCID: PMC2819113.
25. Henry TC, Brynildsen MP. Development of Persister-FACSeq: a method to massively parallelize quantification of persister physiology and its heterogeneity. Sci Rep. 2016;6:25100. doi: 10.1038/srep25100. PubMed PMID: 27142337; PMCID: PMC4855238.
26. Solopova A, van Gestel J, Weissing FJ, Bachmann H, Teusink B, Kok J, Kuipers OP. Bet-hedging during bacterial diauxic shift. Proc Natl Acad Sci U S A. 2014;111(20):7427-32. doi: 10.1073/pnas.1320063111. PubMed PMID: 24799698; PMCID: PMC4034238.
27. Wang J, Chen L, Chen Z, Zhang W. RNA-seq based transcriptomic analysis of single bacterial cells. Integr Biol (Camb). 2015;7(11):1466-76. doi: 10.1039/c5ib00191a. PubMed PMID: 26331465.
28. Wang B, Zhu J, Pierson E, Ramazzotti D, Batzoglou S. Visualization and analysis of single-cell RNA-seq data by kernel-based similarity learning. Nat Methods. 2017;14(4):414-6. doi: 10.1038/nmeth.4207. PubMed PMID: 28263960.
29. Ahidjo BA, Kuhnert D, McKenzie JL, Machowski EE, Gordhan BG, Arcus V, Abrahams GL, Mizrahi V. VapC toxins from Mycobacterium tuberculosis are ribonucleases that differentially inhibit growth and are neutralized by cognate VapB antitoxins. PLoS One. 2011;6(6):e21738. doi: 10.1371/journal.pone.0021738. PubMed PMID: 21738782; PMCID: PMC3126847.
30. Suzuki R, Shimodaira H. Pvclust: an R package for assessing the uncertainty in hierarchical clustering. Bioinformatics. 2006;22(12):1540-2. doi: 10.1093/bioinformatics/btl117. PubMed PMID: 16595560.
31. Ramage HR, Connolly LE, Cox JS. Comprehensive functional analysis of Mycobacterium tuberculosis toxin-antitoxin systems: implications for pathogenesis, stress responses, and evolution. PLoS Genet. 2009;5(12):e1000767. doi: 10.1371/journal.pgen.1000767. PubMed PMID: 20011113; PMCID: PMC2781298.
32. Sala A, Bordes P, Genevaux P. Multiple toxin-antitoxin systems in Mycobacterium tuberculosis. Toxins (Basel). 2014;6(3):1002-20. doi: 10.3390/toxins6031002. PubMed PMID: 24662523; PMCID: PMC3968373.
33. Keren I, Minami S, Rubin E, Lewis K. Characterization and transcriptome analysis of Mycobacterium tuberculosis persisters. MBio. 2011;2(3):e00100-11. doi: 10.1128/mBio.00100-11. PubMed PMID: 21673191; PMCID: PMC3119538.
34. McKenzie JL, Robson J, Berney M, Smith TC, Ruthe A, Gardner PP, Arcus VL, Cook GM. A VapBC toxin-antitoxin module is a posttranscriptional regulator of metabolic flux in mycobacteria. J Bacteriol. 2012;194(9):2189-204. doi: 10.1128/JB.06790-11. PubMed PMID: 22366418; PMCID: PMC3347065.

35. Winther KS, Gerdes K. Regulation of enteric vapBC transcription: induction by VapC toxin dimer-breaking. Nucleic Acids Res. 2012;40(10):4347-57. doi: 10.1093/nar/gks029. PubMed PMID: 22287572; PMCID: PMC3378870.
36. Schifano JM, Edifor R, Sharp JD, Ouyang M, Konkimalla A, Husson RN, Woychik NA. Mycobacterial toxin MazF-mt6 inhibits translation through cleavage of 23S rRNA at the ribosomal A site. Proc Natl Acad Sci U S A. 2013;110(21):8501-6. doi: 10.1073/pnas.1222031110. PubMed PMID: 23650345; PMCID: PMC3666664.
37. Germain E, Roghanian M, Gerdes K, Maisonneuve E. Stochastic induction of persister cells by HipA through (p)ppGpp-mediated activation of mRNA endonucleases. Proc Natl Acad Sci U S A. 2015;112(16):5171-6. doi: 10.1073/pnas.1423536112. PubMed PMID: 25848049; PMCID: PMC4413331.
38. Haseltine WA, Block R. Synthesis of guanosine tetra- and pentaphosphate requires the presence of a codon-specific, uncharged transfer ribonucleic acid in the acceptor site of ribosomes. Proc Natl Acad Sci U S A. 1973;70(5):1564-8. PubMed PMID: 4576025; PMCID: PMC433543.
39. Weiss LA, Stallings CL. Essential roles for Mycobacterium tuberculosis Rel beyond the production of (p)ppGpp. J Bacteriol. 2013;195(24):5629-38. doi: 10.1128/JB.00759-13. PubMed PMID: 24123821; PMCID: PMC3889611.
40. Klinkenberg LG, Lee JH, Bishai WR, Karakousis PC. The stringent response is required for full virulence of Mycobacterium tuberculosis in guinea pigs. J Infect Dis. 2010;202(9):1397-404. doi: 10.1086/656524. PubMed PMID: 20863231; PMCID: PMC2949470.
41. Chatterji D, Ojha AK. Revisiting the stringent response, ppGpp and starvation signaling. Curr Opin Microbiol. 2001;4(2):160-5. PubMed PMID: 11282471.
42. Kriel A, Bittner AN, Kim SH, Liu K, Tehranchi AK, Zou WY, Rendon S, Chen R, Tu BP, Wang JD. Direct regulation of GTP homeostasis by (p)ppGpp: a critical component of viability and stress resistance. Mol Cell. 2012;48(2):231-41. doi: 10.1016/j.molcel.2012.08.009. PubMed PMID: 22981860; PMCID: PMC3483369.
43. Dahl JL, Kraus CN, Boshoff HI, Doan B, Foley K, Avarbock D, Kaplan G, Mizrahi V, Rubin H, Barry CE, 3rd. The role of RelMtb-mediated adaptation to stationary phase in long-term persistence of Mycobacterium tuberculosis in mice. Proc Natl Acad Sci U S A. 2003;100(17):10026-31. doi: 10.1073/pnas.1631248100. PubMed PMID: 12897239; PMCID: PMC187750.
44. Harms A, Fino C, Sorensen MA, Semsey S, Gerdes K. Prophages and Growth Dynamics Confound Experimental Results with Antibiotic-Tolerant Persister Cells. MBio. 2017;8(6). doi: 10.1128 /mBio.01964-17. PubMed PMID: 29233898; PMCID: PMC5727415.
45. Vilcheze C, Hartman T, Weinrick B, Jain P, Weisbrod TR, Leung LW, Freundlich JS, Jacobs WR, Jr. Enhanced respiration prevents drug tolerance and drug resistance in Mycobacterium tuberculosis. Proc Natl Acad Sci U S A. 2017;114(17):4495-500. doi: 10.1073/pnas.1704376114. PubMed PMID: 28396391; PMCID: PMC5410800.
46. Wu ML, Gengenbacher M, Chung JC, Chen SL, Mollenkopf HJ, Kaufmann SH, Dick T. Developmental transcriptome of resting cell formation in Mycobacterium smegmatis. BMC Genomics. 2016;17(1):837. doi: 10.1186/s12864-016-3190-4. PubMed PMID: 27784279; PMCID: PMC5081680.

47. Raj A, van Oudenaarden A. Nature, nurture, or chance: stochastic gene expression and its consequences. Cell. 2008;135(2):216-26. doi: 10.1016/j.cell.2008.09.050. PubMed PMID: 18957198; PMCID: PMC3118044.
48. Avery SV. Microbial cell individuality and the underlying sources of heterogeneity. Nat Rev Microbiol. 2006;4(8):577-87. doi: 10.1038/nrmicro1460. PubMed PMID: 16845428.
49. Dhar N, McKinney JD. Microbial phenotypic heterogeneity and antibiotic tolerance. Curr Opin Microbiol. 2007;10(1):30-8. doi: 10.1016/j.mib.2006.12.007. PubMed PMID: 17215163.
50. Korch SB, Henderson TA, Hill TM. Characterization of the hipA7 allele of Escherichia coli and evidence that high persistence is governed by (p)ppGpp synthesis. Mol Microbiol. 2003;50(4):1199-213. PubMed PMID: 14622409.
51. Bhaskar A, De Piano C, Gelman E, McKinney JD, Dhar N. Elucidating the role of (p)ppGpp in mycobacterial persistence against antibiotics. IUBMB Life. 2018;70(9):836-44. doi: 10.1002/iub.1888. PubMed PMID: 30092117.
52. Verstraeten N, Knapen WJ, Fauvart M, Michiels J. Membrane depolarization-triggered responsive diversification leads to antibiotic tolerance. Microb Cell. 2015;2(8):299-301. doi: 10.15698/mic2015.08.220. PubMed PMID: 28357305; PMCID: PMC5349102.
53. Marques CN, Morozov A, Planzos P, Zelaya HM. The fatty acid signaling molecule cis-2-decenoic acid increases metabolic activity and reverts persister cells to an antimicrobial-susceptible state. Appl Environ Microbiol. 2014;80(22):6976-91. doi: 10.1128/AEM.01576-14. PubMed PMID: 25192989; PMCID: PMC4249009.
54. Courtney CM, Goodman SM, Nagy TA, Levy M, Bhusal P, Madinger NE, Detweiler CS, Nagpal P, Chatterjee A. Potentiating antibiotics in drug-resistant clinical isolates via stimuli-activated superoxide generation. Sci Adv. 2017;3(10):e1701776. doi: 10.1126/sciadv.1701776. PubMed PMID: 28983513; PMCID: PMC5627983.
55. Wexselblatt E, Oppenheimer-Shaanan Y, Kaspy I, London N, Schueler-Furman O, Yavin E, Glaser G, Katzhendler J, Ben-Yehuda S. Relacin, a novel antibacterial agent targeting the Stringent Response. PLoS Pathog. 2012;8(9):e1002925. doi: 10.1371/journal.ppat.1002925. PubMed PMID: 23028324; PMCID: PMC3447753.

56. Parikh A, Kumar D, Chawla Y, Kurthkoti K, Khan S, Varshney U, et al. Development of a New Generation of Vectors for Gene Expression, Gene Replacement, and Protein-Protein Interaction Studies in Mycobacteria. Appl Environ Microbiol. 2013 Mar;79(5):1718–29.

57. McKinney SA, Murphy CS, Hazelwood KL, Davidson MW, Looger LL. A bright and photostable photoconvertible fluorescent protein for fusion tags. Nat Methods. 2009 Feb;6(2):131–3.

58. Carroll P, Schreuder LJ, Muwanguzi-Karugaba J, Wiles S, Robertson BD, Ripoll J, et al. Sensitive Detection of Gene Expression in Mycobacteria under Replicating and Non-Replicating Conditions Using Optimized Far-Red Reporters. PLOS ONE. 2010 Mar 23;5(3):e9823.

688 59. Bonev B, Hooper J, Parisot J. Principles of assessing bacterial susceptibility to antibiotics
689 using the agar diffusion method. J Antimicrob Chemother. 2008 Jun 1;61(6):1295–301.

690 60. Baldi P, Long AD. A Bayesian framework for the analysis of microarray expression data:
691 regularized t -test and statistical inferences of gene changes. Bioinforma Oxf Engl. 2001
692 Jun;17(6):509–19.

693
694

695

Figures and tables:

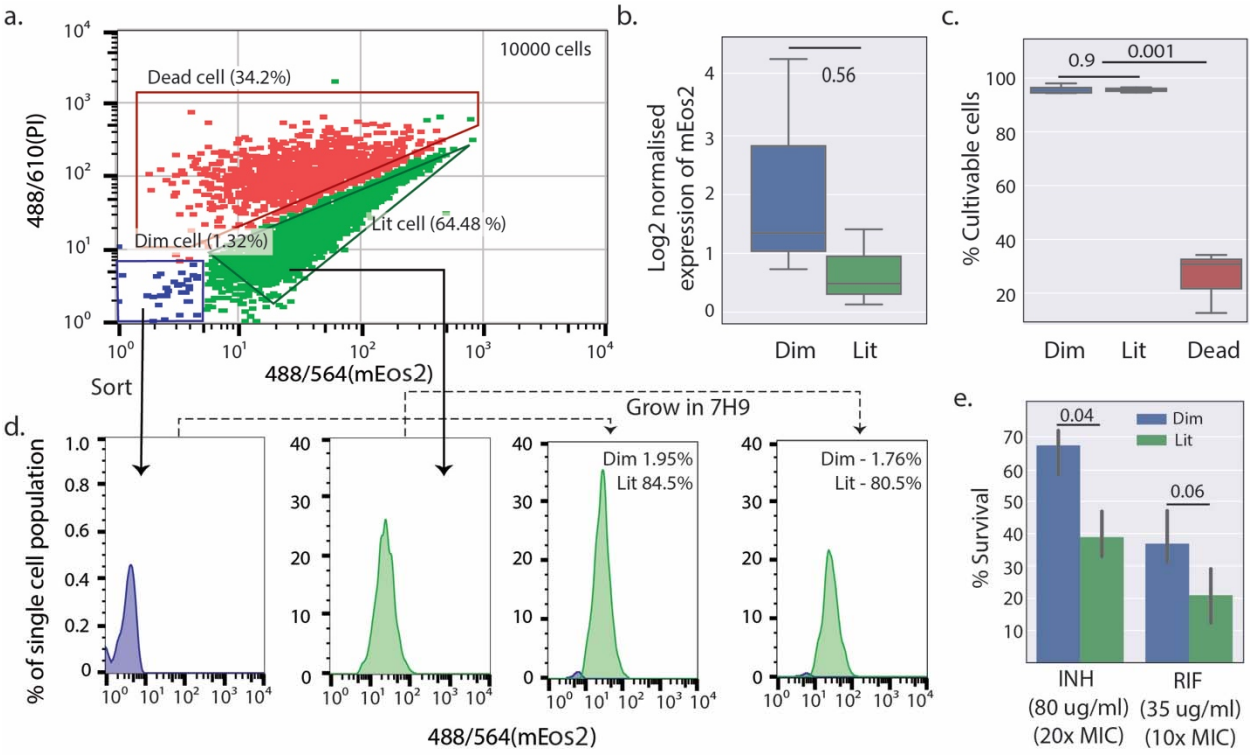

Figure 1: Preexisting translationally dormant population of *Mycobacterium* culture are persisters. (**a**) Fluorescence intensity of mEos2 protein in MSM-mEos2 strain induced with 25 ng/μl of ATc. Population structure was observed in FACS after 12 hours of induction at OD 1.0. Populations are colored and annotated based on the FACS gates described in **Fig S1b**. The polygons in the plot are the gates from which the fractions were sorted for analyses described in this study. (**b**) mEOS2 transcript levels derived from ΔΔCt values obtained by qRT-PCR, values were subtracted from genomic DNA signal and normalized to control gene (see materials and methods for details). (**c**) Cultivability of live cells subpopulations (lit and dim) compared to dead cells. Cultivability was measured as ratio of number of cell forming units (CFU) and number of cells sorted. (**d**) Dim and lit cells (1,000 per) were collected from gates marked in **Fig 1a**. Sorted subpopulations were regrown in 7H9 media until OD_{600} reached 0.6 and then induced with 25 ng/µl of ATc. Induced cultures were observed in FACS (dotted line) and dim and lit percentages were determined from gates described in **Fig 1a**. (**e**) FACS sorted dim and lit cells were treated with 20x MIC INH and 10x MIC RIF for 8 hours before they were washed and plated onto 7H10 plates to determine percentage survival (difference in CFUs compared to 0 hour incubation).

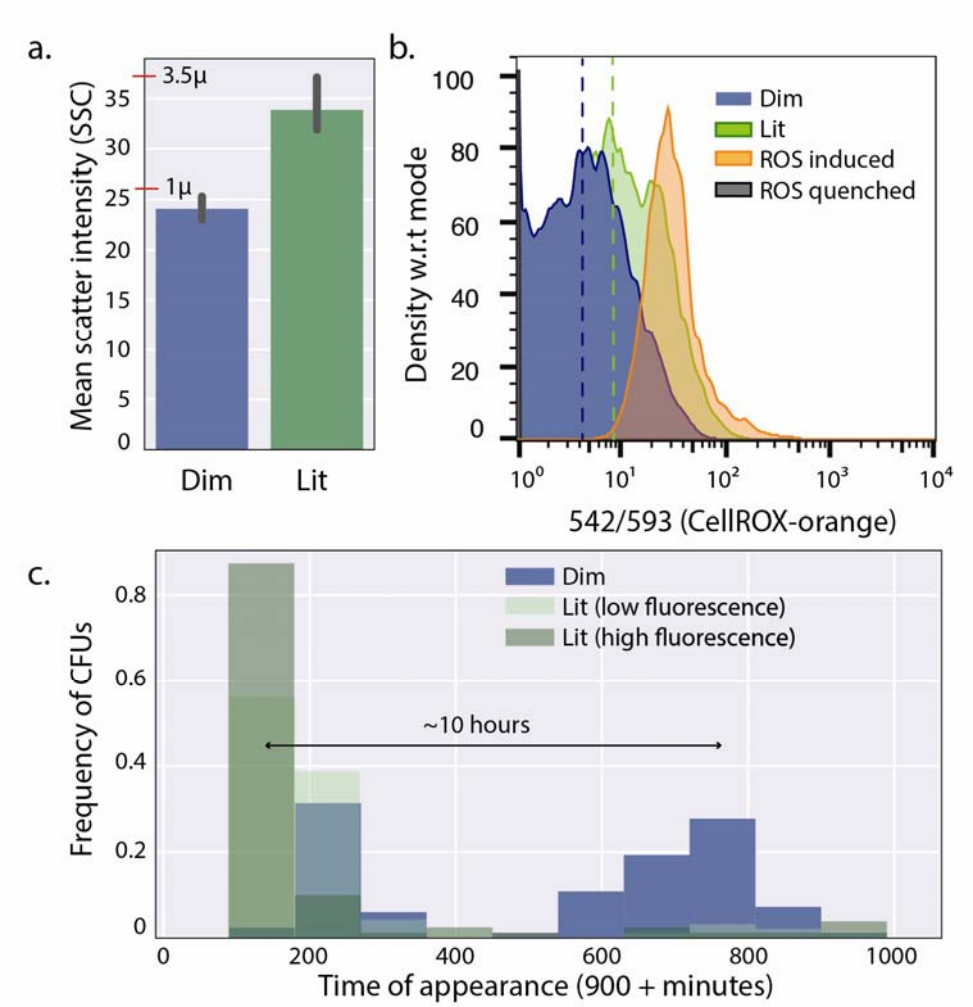

Figure 2: Increased lag phase, slow growth and metabolic dormancy of persisters aid in tolerance to antibiotics. (**a**) Scatter intensity of dim and lit cells obtained from gates described in **Fig1a**, red lines on y axis represents mean scatter intensity of fluorescent beads of size 1µm and 3.5µm. (**b**) CellRox-orange intensity, indicative of cellular ROS levels and oxidative state, was measured after incubating ATc induced MSM-mEos2 strain in CellRox-orange (5 µM/ml) for 2 hours. MSM-mEos2 cells incubated in 100 µM TBHP and 2000 µM NAC (3 hours) was used as positive control (ROS induced, orange) and negative controls (ROS quenched, grey), respectively. *Note: Histogram of ROS-quenched cells is shifted in its entirety to zero CellROX-orange fluorescence, appearing as a line along the y-axis, and hence is not clearly visible in the plot.* (**c**) Lag phase of Per-Sorted dim, high and low fluorescing lit cells (100 cells, gates described in **Fig 1a**) was determined by measuring time of appearance (TOA) of colonies on 7H10 plates supplemented with 0.5% glycerol and OADC, incubated at 37°C. Arrow indicates difference in average TOA of dim and lit (high and low fluorescing) population.

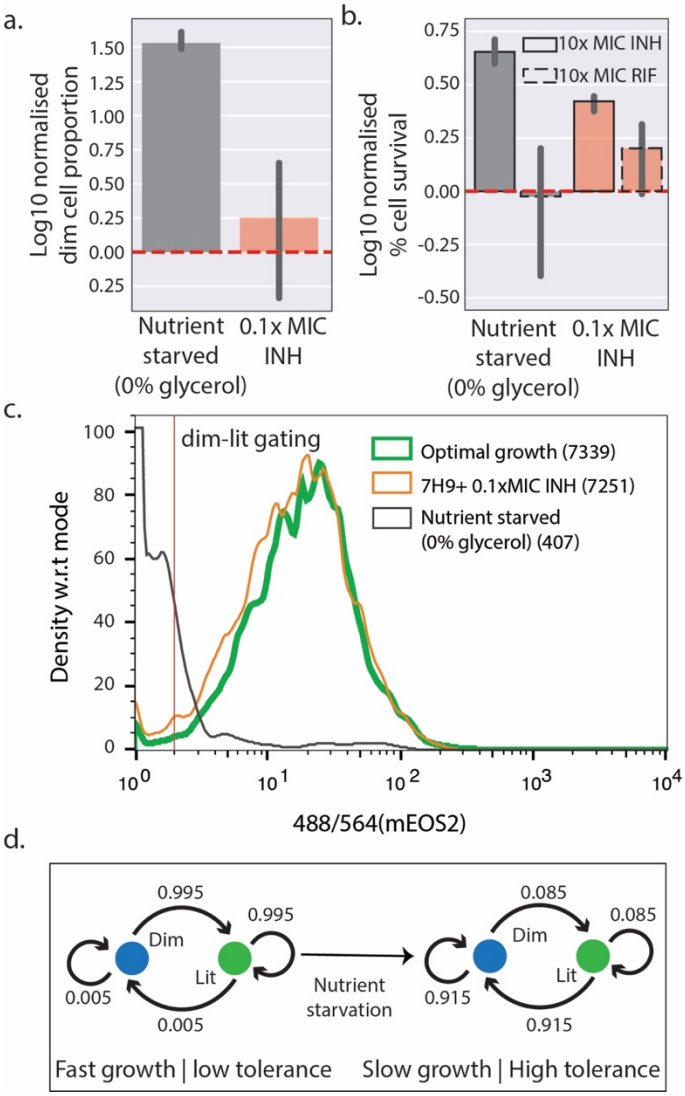

Figure 3: Nutrient starvation induces anticipated stochastic switching of persisters. MSM-mEos2 cultures were grown in 7H9 (0.5% glycerol), 7H9 (0.5% glycerol) + 0.1x MIC INH, and nutrient starvation (PBS, 0% glycerol) conditions. Cultures were induced with ATc (25ng/ul) and dim cell proportions were determined with Per-Sort (a) and other half on same cultures was incubated in 10xMIC INH (40 µg/ml) and 10x MIC RIF (35 µg/ml) (RIF) for 12 hours , washed and plated to determine tolerance similar to **Fig 1e**. Dashed red line indicates dim cell proportions and tolerance of cultures grown in 7H9 at optimal growth conditions. (c) Density of mEos2 fluorescence intensity with respect to mode of the population in live cells of cultures grown in varying conditions mentioned in **Fig 3a,b**. Number of live single cell observed per 10000 cells observed in Per-Sort assay is mentioned in the parenthesis (d) Bet-hedging model with probabilistic conversions between dim and lit cells observed in the MSM cultures under normal and nutrient starved conditions.

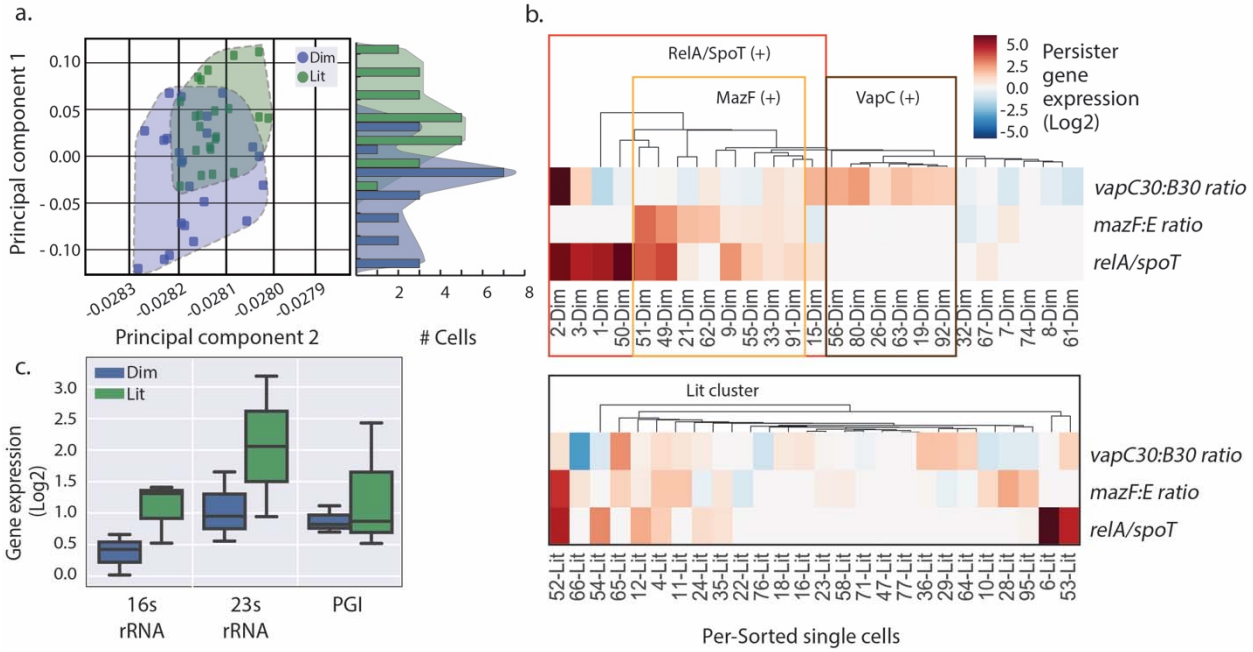

Figure 4: Overexpressed toxin genes and active alarmone response drive stochastic formation of pre-existing persisters. (a) kPCA plot of dim and lit subpopulation performed with persister gene expression and TA ratio of single-cells sorted with Per-Sort method. Shaded regions in the kPCA plot represent area spanned by single cells of respective subpopulation. Histogram to the right is drawn by binning the population by their principle component 1 values and shaded region is drawn by connecting modes at every bin. (b) Persister gene expression based sub clusters in Per-Sorted dim and Lit subpopulation. Boxes indicate cell clusters with AU/BP value > 90%. Clusters were deemed significant if cell number in cluster > 4 cells (10% of subpopulation used in assay). (c) rRNA expression levels in Dim and Lit subpopulation determined by qRTPCR from 100,000 Per-Sorted dim and lit cells. The metabolic gene *phospho-glucoisomerase* (PGI) transcript was used as reference.

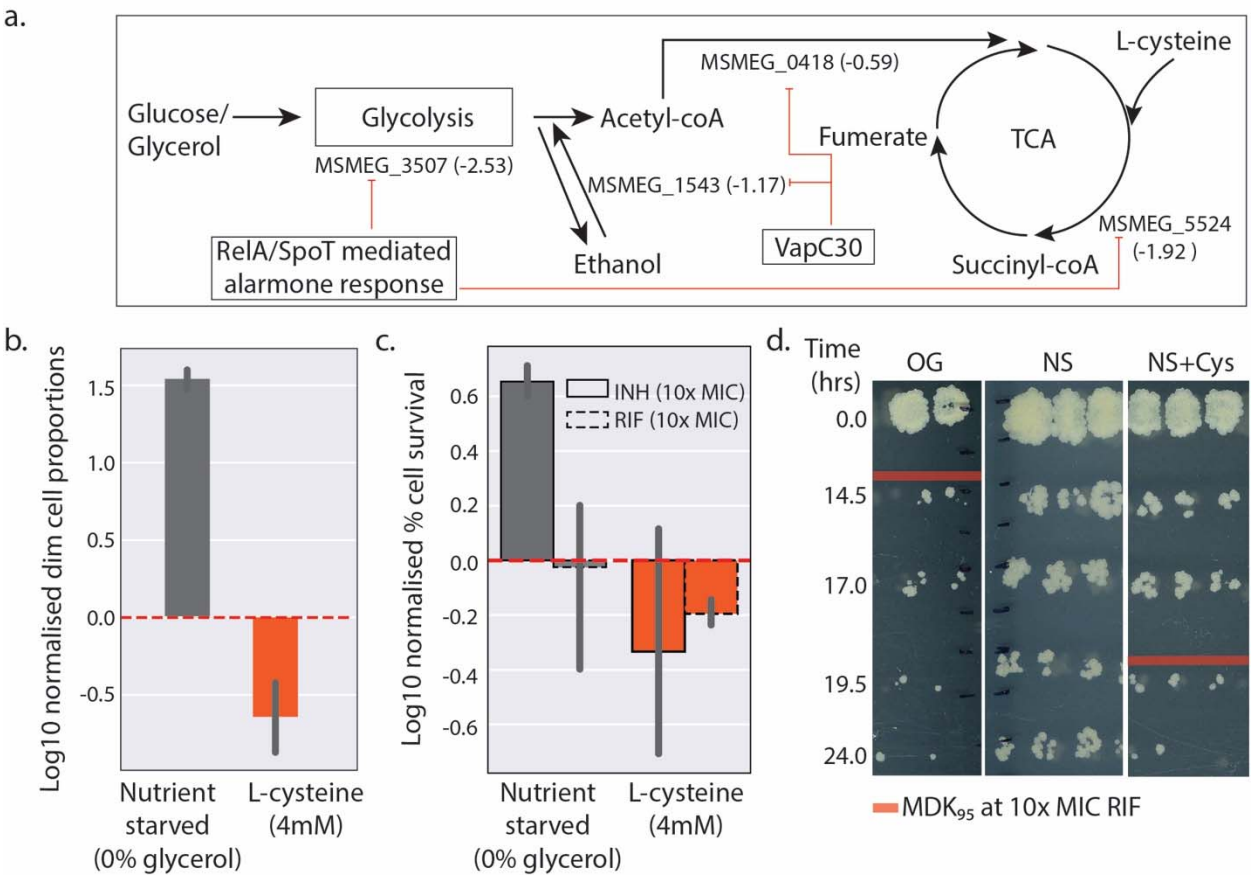

Figure 5: L-cysteine potentiates persister killing. Cultures were incubated in 7H9(Kan$^+$), PBS(Kan$^+$) (Nutrient starvation- NS), and 7H9(Kan$^+$) with 4mM L-cysteine (Cys). (**a**) Effects of VapC30 over expression and RelA/SpoT mediated alarmone response on central carbon metabolism determined by pathway analysis (see methods), Repressing (red edges with bars) influences were derived from transcriptome analysis of GSE29631, GSE69681, and GSE69983 GEO gene expression datasets. Values in parentheses indicate magnitude of effect (log2 fold change). See Methods for details (**b-c**) Dim cell proportions and drug tolerance to INH and RIF of cultures grown in nutrient starved condition (NS) and in presence of L-cysteine (Cys). Assay was performed with method described in **Fig 3a-b** and values were normalized to cultures grown in 7H9. (**d**) Potentiator activity of L-cysteine was determined by adding L-cysteine along with 10x MIC RIF (30 µg/ml) to nutrient starved cultures (NS, NS+Cys). Cultures were diluted in 7H9 media (1:100) and spotted onto 7H10 plates at varying time points to determine the MDK_{95} (Red line). Cultures grown in 7H9 at optimal growth conditions (OG) were used as reference.

Supplementary figures and tables-

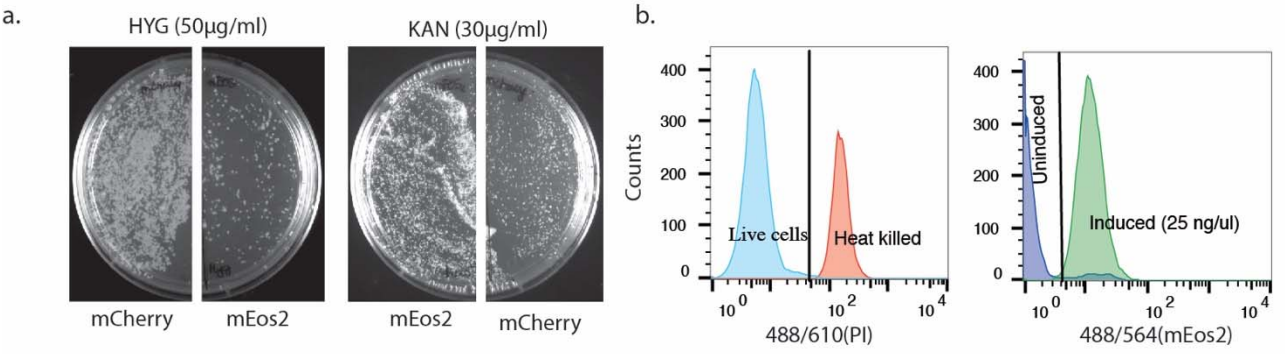

Supplementary figure1: (a) Efficiency in bacterial single cell sorting demonstrated by sorting equal-mixture of *M. smegmatis* with mCherry-Hyg^R and mEos2-Kan^R strains. Sorted cells plated on 7H10+HYG (right panel) and 7H10+KAN (left panel) plates. Plating shows 95% efficiency in single cell sorting. (b) Gating strategies used in identification of dim cells. Gating between PI stained live and dead mEos2 strains (left panel), and PI stained non-fluorescing uninduced and ATc (25ng/µl) induced mEos2 strains (right panel).

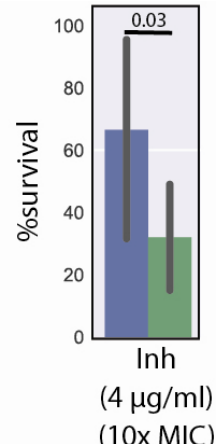

Supplementary figure2: Tolerance of PER-sorted dim and lit cells of *M. tuberculosis*-mEos2 strain to 10x MIC INH measured after 3 days similar to **fig1e**.

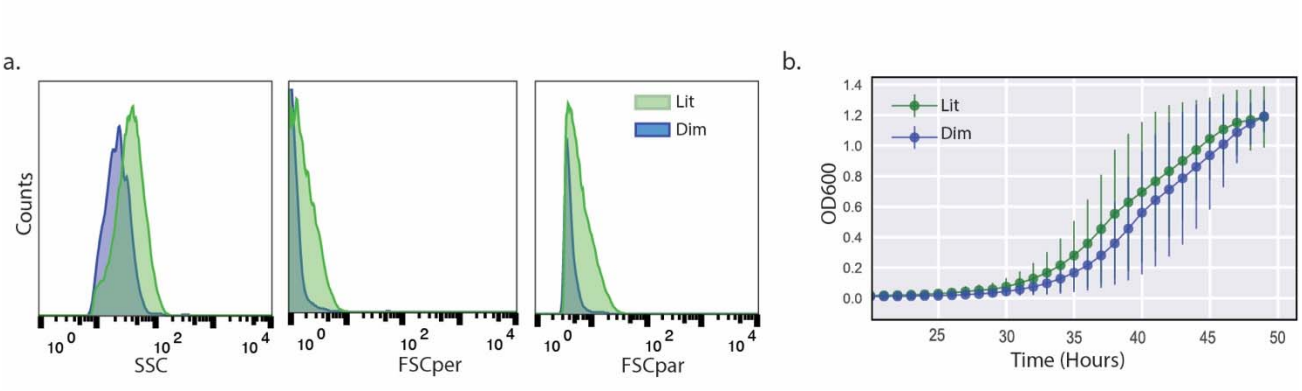

Supplementary figure3: (a) Comparison of scatter intensities of PER-sorted dim and lit cells in *M. smegmatis*. (b) Growth curve of PER-sorted 1000 *M. smegmatis*-mEos2 dim and lit cells measured as optical density at 600 nm.

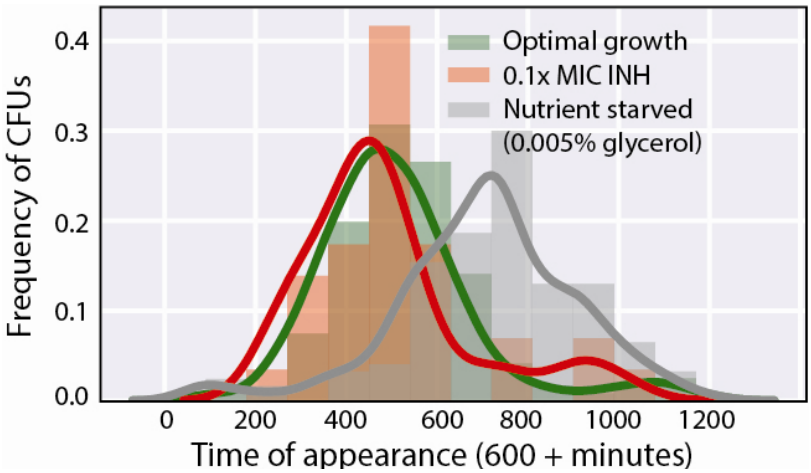

Supplementary figure4: Time of appearance of colonies in cultures grown in optimal growth media (7H9 with 0.2% glycerol), 7H9 + 0.1x MIC INH, and nutrient starved media (7H9 with 0.005% glycerol).

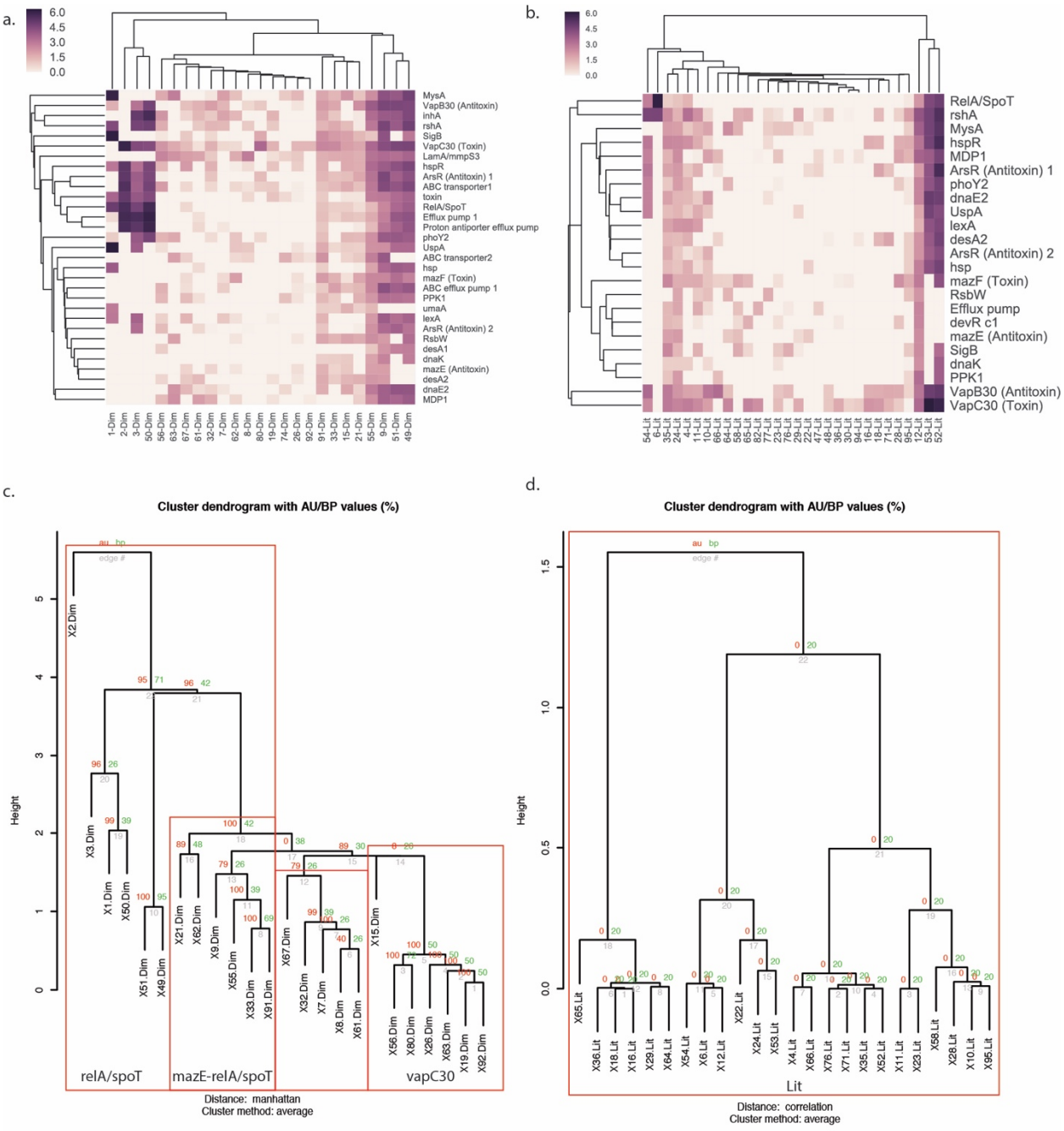

Supplementary figure5: (a,b) Hierarchical clustering of single cell persister gene expression for dim (a) and lit (b) subpopulation. (c,d) Hierarchical clustering with PV clust based on *relA/spoT* expression and TA ratio of *vapC30:vapB30* and *mazF:E* of per-Sorted dim (c) and lit (d) Clusters were assigned for nodes with AU/BP value > 90% and > 4 cells (10% of sub-population used in assay). Clusters were named based on their highly expressed gene or pathway.

815 **Supplementary table1**: Genes used in single cell persister gene expression assay
816

MSM gene ID	Gene name	Gene function
MSMEG_2817	ABC efflux pump 1	ABC efflux pump 1
MSMEG_5659	ABC transporter1	ABC transporter1
MSMEG_5660	ABC transporter2	ABC transporter2
MSMEG_3945	ABC transporter3	ABC transporter3
MSEMG_2740	lexA	Alarmone response
MSMEG_2965	relA/spoT	Alarmone response
MSMEG_2391	ppk1	Alarmone response
ECC2_spikein RNA	Assay control	Control
PBR372 region of pstKi mEOS2	Genomic DNA control	Control
MSMEG_1633	dnaE2	DNA replication
MSMEG_3151	inhA	Drug target
MSMEG_2723	RecA	Drug target
MSMEG_4427	Efflux pump 1	Efflux pump 1
MSMEG_3944	devR c1	Metabolic control
MSMEG_6384	katG	Metabolic control
MSMEG_5244	devR c2	Metabolic control
MSMEG_1605	phoY1	Persister phenotype associated gene
MSMEG_5776	phoY2	Persister phenotype associated gene
MSMEG_1915	rshA	Persister phenotype associated gene
MSMEG_4265	lamA/mmpS3	Persister phenotype associated gene
MSMEG_0913	umaA	Persister phenotype associated gene
MSMEG_5773	desA1	Persister phenotype associated gene
MSMEG_0916	desR	Persister phenotype associated gene
MSMEG_5248	desA2	Persister phenotype associated gene
MSMEG_0424	hsp	Persister phenotype associated gene
MSMEG_4466	uspA	Persister phenotype associated gene
MSMEG_5141	narK2	Persister phenotype associated gene
MSMEG_1803	rsbW	Persister phenotype associated gene
MSMEG_6225	Proton antiporter efflux pump	Proton antiporter efflux pump
MSMEG_2389	mdp1	Regulator
MSMEG_0709	dnaK	Regulator
MSMEG_2752	SigB	Sigma factor
MSMEG_1914	rpoE1	Sigma factor
MSMEG_2758	mysA	Sigma factor

MSMEG_0713	hspR	Sigma factor
MSMEG_1277	un-annotated	TA operon (Antitoxin)
MSMEG_1283	vapB30 (Antitoxin)	TA operon (Antitoxin)
MSMEG_3180	antitoxin	TA operon (Antitoxin)
MSMEG_4175	arsR (Antitoxin) 1	TA operon (Antitoxin)
MSMEG_4447	mazE (Antitoxin)	TA operon (Antitoxin)
MSMEG_6762	arsR (Antitoxin) 2	TA operon (Antitoxin)
MSMEG_1278	Un-annotated	TA operon (Toxin)
MSMEG_1284	vapC30 (Toxin)	TA operon (Toxin)
MSMEG_3181	toxin	TA operon (Toxin)
MSMEG_4176	arsR (Toxin) 1	TA operon (Toxin)
MSMEG_4448	mazF (Toxin)	TA operon (Toxin)
MSMEG_6760	arsR (Toxin) 2	TA operon (Toxin)

817
818

819 **Supplementary table2** : Primers used in the study

820

MSM gene ID	FP	RP
MSMEG_1277	GGCGGATGACCTGTCGCTGA	GGCGACCCTGCGCTTGTG
MSMEG_1278	CCATGCGCTGGTCGACGGTA	TCCTCCGCGCGATCGACATC
MSMEG_1283	GAGGCGGTGGTGATGGCACT	GAGGCGGTGGTGATGGCACT
MSMEG_1284	GCGGTGGCTGACGATCCTGT	GAGTTCGCGACCACCTGGCT
MSMEG_3180	TCGCGGTGCTCATGGACGAC	CGGGCACGTGCACTGCATTC
MSMEG_3181	CCGGACGCGGTCTACGTGTT	AAGCTCACCCGCACGATCCC
MSMEG_4175	TGCCCTGGTCGACGGTGAAC	GACCTCGCGCAGCACCTTGA
MSMEG_4176	GGCACGGTGCTTCGCTTCAC	CGGTCGAAGAAGGCGTGGGT
MSMEG_4447	ACCGAGTACGCCGACATCGC	GGCGGCGACCAACTCAGACT
MSMEG_4448	AATCGAGCCAACGCCAGCCA	CGACACGGTGCGTCAAGCTG
MSMEG_6760	CCCGGACGGCGAGAAGTACG	AGCGAACCCGTCGAGGAACG
MSMEG_6762	CACGAGGCGCGACATCATGC	AGCAGGCCGGCTTTCTCCAG
MSMEG_2694	CACTTTCGCGCGTGCTCACC	GCCATGGACACCTGCGGGAT
MSMEG_4671	GATCGCCCGCAAGAGCGAGA	GACGCCTGCGTACCCTCCAG
MSMEG_4466	CGGTTCCGCCACATCACCCT	GGTGAGCGCGTAGACGGTGT
MSMEG_1803	GTGGATCCCGGTCCCGATGC	CAGGCCCGGACCCATCTGTG
MSMEG_1633	AGTGGGCCCGCATGGAGAAC	CCGAGGCCCAGCATGTCGAA
MSMEG_6384	CCGGTGAGCGTGACCTGGAG	TGCGGATCCGGATTGCCGTT
MSMEG_2389	CACAGAAGCTCCCGGCCGAT	CACAGAAGCTCCCGGCCGAT
MSMEG_3151	TCGACGGTGTGGTGCACTCG	GCGCGTCGAAGAACGGGTTG
MSMEG_2723	CAGGCGCTGCGCAAGATGAC	CTCGGGCGAGCCGAACATCA
MSMEG_2740	GACACCGGCGAGTTCACGGA	TCGAGGATGGTGCGCTGACG
MSMEG_2965	GTGCTCGCCGACGAGAAGGT	GTGCTTCGGGTCGCCCATCT
MSMEG_1915	GCCTGCGGCATTACGGCATC	TCGTGGTGCGGCTGATCTGG
MSMEG_4265	GCCGACGTGGCGCTCTATGA	GCCGACGTGGCGCTCTATGA
MSMEG_5659	TGGCGTCTCGGCCTGATGTG	TACGTGCGGGCGGATTCGTT
MSMEG_0913	GGAAGTCCGCCTGCAGGGTT	GGGTAGCGCTCGGCCTTGAA
MSMEG_5660	GTCGACCATCCGCCGGTTCA	CAGCAGGATCGCGGTGACCA
MSMEG_0709	GCGACCTCCGGTGACAACCA	GATGCCCGAGCTGCCCTTGA
MSMEG_0424	AATCCGACGGCCGCACCTAC	CCGGCGACCCGTACCTTCAG
MSMEG_0713	ACCTGCTGCGAGAGGTGCAG	AGCGCGTCGACCTGATTGGT
MSMEG_3932	CATGCGCTCGGTGACACTGC	TCTCCACCGCGACACGCTTC
MSMEG_5141	GGTCGGATCGTTGGGACGCA	CAGGATCGACGCGACCGTCA
MSMEG_3945	ATCCACGGCGAGTCGAAGGC	CGTCGAGAGGCTGCGTCGAA
MSMEG_0880	GGTCGGCAACGAGGGTGTCA	CTCGGCGTCGGTCACGAAGT
MSMEG_1583	CATCGCCGATCGCGTCAAGC	AGCCGCTCCTGCAGCTTCTC

MSMEG_2391	GCTGTTGGAGCGCGCGAAAT	AGCGCACCGACAGACCCATC
MSMEG_3944	CGACCCGAAGTCGCGGTTCT	GTGGCCTCGTCGGACGTGAA
MSMEG_5244	TCACCCAGCAGGAGCGTGTG	CGCGCCGCGATCTGTTTGTT
MSMEG_1605	CCGATCTGACGCTGGCCGAA	GTGCATGGACCCGACGACCA
MSMEG_5776	CACGCGGGATCCGGAGAAGG	CCACTCGCGGTCCATCAGCA
MSMEG_2752	TCGACATGCCGGTCGGAACC	GGCGGACATGGCCTCGGAAT
MSMEG_1914	GTCCAACGCCGAGCACTCCT	GCTTGCAACGCGGCCTTGAT
MSMEG_2758	AGGGCGAGAAGCTGCCAGTG	GCAGGTTCGCCTCCAGCAGA
MSMEG_2817	TGGGAGCCGCTGGCTTCTAC	CCGACGACGGTACCGAGGAA
MSMEG_4427	GCGGTTTGGCTTCCGCAGTC	GCGGCGCTGACCTTCAACAC
MSMEG_6225	GGGTGCCGTGGTGTCGATGA	CCAGGCCCGTGACCATCAGG
MSMEG_5773	GGCCTCGACATCGCGCCGAA	GCGGAGCACCGGCATCACGA
MSMEG_0916	CCGTCGGCGGTGTCCAGCTC	ATGCCGCACAGCGCGTACCA
MSMEG_5248	GCGGGCCTCGACGTGATCGG	CTCGGCGACGTTGGCGACCT
Assay control (Spike in)	TCCAGATTACTTCCATTTCCGC	GCTGGATGCCGACGCCCGTAT
Genomic DNA control (NT region)	TGGCTGCTGCCAGTGGCGAT	GCCCGACCGCTGCGCCTTAT

821
822
823
824
825
826